# “Photonic lantern” spectral filters in multi-core fibre

**T. A. Birks,[1,*] B. J. Mangan,[1] A. Díez,[2] J. L. Cruz,[2] and D. F. Murphy[3]**

[1]*Department of Physics, University of Bath, Claverton Down, Bath, BA2 7AY, UK*
[2]*Departamento de Física Aplicada-ICMUV, Universidad de Valencia, Dr Moliner 50, 46100 Burjasot, Spain*
[3]*Waterford Institute of Technology, Waterford, Ireland*
[*]*t.a.birks@bath.ac.uk*

**Abstract:** Fibre Bragg gratings are written across all 120 single-mode cores of a multi-core optical fibre. The fibre is interfaced to multimode ports by tapering it within a depressed-index glass jacket. The result is a compact multimode “photonic lantern” filter with astrophotonic applications. The tapered structure is also an effective mode scrambler.



**OCIS codes:** (060.2280) Fiber design and fabrication; (060.3735) Fiber Bragg gratings; (060.2340) Fiber optics components; (350.1260) Astronomical optics.

## References and links

1. S. G. Leon-Saval, T. A. Birks, J. Bland-Hawthorn, and M. Englund, “Multimode fiber devices with single-mode performance,” Opt. Lett. **30**(19), 2545–2547 (2005).
2. D. Noordegraaf, P. M. W. Skovgaard, M. D. Nielsen, and J. Bland-Hawthorn, “Efficient multi-mode to single-mode coupling in a photonic lantern,” Opt. Express **17**(3), 1988–1994 (2009).
3. S. G. Leon-Saval, A. Argyros, and J. Bland-Hawthorn, “Photonic lanterns: a study of light propagation in multimode to single-mode converters,” Opt. Express **18**(8), 8430–8439 (2010).
4. J. Bland-Hawthorn, S. C. Ellis, S. G. Leon-Saval, R. Haynes, M. M. Roth, H.-G. Löhmannsröben, A. J. Horton, J.-G. Cuby, T. A. Birks, J. S. Lawrence, P. Gillingham, S. D. Ryder, and C. Trinh, “A complex multi-notch astronomical filter to suppress the bright infrared sky,” Nat Commun **2**, 581 (2011).
5. J. Bland-Hawthorn, M. Englund, and G. Edvell, “New approach to atmospheric OH suppression using an aperiodic fibre Bragg grating,” Opt. Express **12**(24), 5902–5909 (2004).
6. R. R. Thomson, T. A. Birks, S. G. Leon-Saval, A. K. Kar, and J. Bland-Hawthorn, “Ultrafast laser inscription of an integrated photonic lantern,” Opt. Express **19**(6), 5698–5705 (2011).
7. G. M. H. Flockhart, W. N. MacPherson, J. S. Barton, J. D. C. Jones, L. Zhang, and I. Bennion, “Two-axis bend measurement with Bragg gratings in multicore optical fiber,” Opt. Lett. **28**(6), 387–389 (2003).
8. C. G. Askins, T. F. Taunay, G. A. Miller, B. M. Wright, J. R. Peele, L. R. Wasserman, and E. J. Friebele, “Inscription of Fiber Bragg Gratings in Multicore Fiber,” in *Nonlinear Photonics*, OSA Technical Digest (CD) (Optical Society of America, 2007), paper JWA39.
9. T. A. Birks, A. Diez, J. L. Cruz, S. G. Leon-Saval, and D. F. Murphy, “Fibers are looking up: optical fibre transition structures in astrophotonics,”in *Frontiers in Optics*, OSA Technical Digest (CD) (Optical Society of America, 2010), paper FTuU1.
10. T. A. Birks, B. J. Mangan, A. Diez, J. L. Cruz, S. G. Leon-Saval, J. Bland-Hawthorn, and D. F. Murphy, “Multicore optical fibres for astrophotonics,”in*CLEO/Europe and EQEC 2011 Conference Digest*, OSA Technical Digest (CD) (Optical Society of America, 2011), paper JSIII2_1.
11. E. Carrasco and I. R. Parry, “A method for determining the focal ratio degradation of optical fibres for astronomy,” Mon. Not. R. Astron. Soc. **271**, 1–12 (1994).
12. A. W. Snyder and J. D. Love, *Optical Waveguide Theory* (Chapman and Hall, 1983).
13. D. Gloge, “Weakly guiding fibers,” Appl. Opt. **10**(10), 2252–2258 (1971).
14. M. Olivero, G. Perrone, and A. Vallan, “Near-field measurements and mode power distribution of multimode optical fibers,” IEEE Trans. Instrum. Meas. **59**(5), 1382–1388 (2010).
15. K. O. Hill, B. Malo, F. Bilodeau, D. C. Johnson, and J. Albert, “Bragg gratings fabricated in monomodephotosensitive optical fiber by UV exposure through a phase mask,” Appl. Phys. Lett. **62**(10), 1035–1037 (1993).
16. H. F. Taylor, “Bending effects in optical fibers,” J. Lightwave Technol. **2**(5), 617–628 (1984).
17. J. D. Love, W. M. Henry, W. J. Stewart, R. J. Black, S. Lacroix, and F. Gonthier, “Tapered single-mode fibres and devices part 1: adiabaticity criteria,” IEEE Proc. Pt. J **138**, 343–354 (1991).
18. BeamPROP by RSoft, *http://www.rsoftdesign.com*.
19. MMF preform supplied by j-fiber, *http://www.j-fiber.com*.

#167650 - $15.00 USD Received 30 Apr 2012; revised 22 May 2012; accepted 28 May 2012; published 8 Jun 2012

20. M. Ohashi, M. Tateda, K. Tajima, and K. Shiraki, "Fluorine concentration dependence of viscosity in F-doped silica glass," Electron. Lett. **28**(11), 1008–1010 (1992).

## 1. Introduction

The photonic lantern is a tapered structure that allows a multimode optical fibre device to take advantage of the performance of single-mode components [1–4]. It was motivated by the need to filter out narrow spectral lines from multimode light delivered by astronomical telescopes, where the single-mode component is a complex fibre Bragg grating (FBG) [5]. The first example combined $N = 19$ individual single-mode (SM) fibres to form one multimode fibre (MMF) core in a photonic crystal fibre cladding [1]. Subsequent work has raised $N$ as high as 61, with low-index F-doped silica glass as the MMF cladding [2–4]. Photonic lanterns with such claddings are now being tested on sky [4]. Nevertheless they are cumbersome and expensive to produce by a specialized tapering process, and require $N$ identical single-mode FBGs to be spliced to twice as many SM fibre pigtails for each device.

Integrated-optic photonic lanterns have also been made by ultrafast laser inscription [6]. This technology is scalable to much greater $N$, offers a variety of other functions and can work at wavelengths that are not transmitted by fused silica. However, such photonic lanterns are at an early stage of development and have yet to be demonstrated with the filtering function. In comparison the fibre approach currently retains advantages of low loss and ready compatibility with fibre-coupled telescope optics.

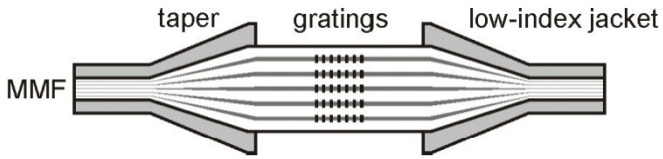


Fig. 1. Schematic of a photonic lantern filter. It is formed from a multicore fibre tapered at both ends in a jacket of low-index glass to form MMF ports. Fibre Bragg gratings are written in the SM cores in the middle section of the MCF.

Here we report a compact, readily-manufacturable prototype of a photonic lantern based on a multi-core fibre (MCF) containing $N = 120$ separate single-mode cores, Fig. 1. Bragg gratings were written in one inscription process across all of the cores at once. (To the authors' knowledge the maximum number of MCF cores into which FBGs had previously been simultaneously inscribed was four [7, 8].) The MCF was tapered within a snug-fitting F-doped silica jacket to produce MMF ports at both ends. The resulting multimode filter had a notch transmission spectrum with a depth of 7 dB and a width of 0.2 nm, against a background insertion loss of <0.5 dB. The notch depth was limited by the uniformity of the gratings across the cores not the quality of the lantern transitions, and should be improved by further development of the multicore FBG inscription process. This form of the photonic lantern was first proposed in 2005 [1] and preliminary experimental results were presented in [9, 10].

The lantern device (without FBGs) was also a very effective MMF mode scrambler, with output near-field intensity distributions that were much more sensitive to perturbations (and so easier to make uniform by time or spectral averaging) than a simple MMF.

## 2. Design

### *2.1 Mode number mismatch loss*

Lossless coupling of light from an input MMF's $N_{in}$ arbitrarily-excited spatial modes into one SM core would decrease the number of degrees of freedom and hence the entropy, and so is forbidden by the second law of thermodynamics [1]. Any left-over degrees of freedom couple to loss. For low loss there must therefore be $N_{SM} \geq N_{in}$ SM cores in the MCF. Similarly, for

#167650 - $15.00 USD Received 30 Apr 2012; revised 22 May 2012; accepted 28 May 2012; published 8 Jun 2012

low-loss coupling from $N_{SM}$ arbitrarily-excited SM cores into an output MMF the MMF must support $N_{out} \geq N_{SM}$ modes. However, allowing $N$ to increase from input to output causes focal ratio degradation (FRD) [11]. A necessary condition for low loss without FRD is therefore that the numbers of modes in each section must match: $N_{SM} = N_{MM}$, where $N_{MM} = N_{in} = N_{out}$.

The approximate number of spatial modes supported by a step-index MMF with core diameter $d_{MM}$ and numerical aperture $NA_{MM}$ for light of wavelength $\lambda$ is given by

$$N_{MM} \approx \frac{V_{MM}^2}{4} = \frac{\pi^2 d_{MM}^2 NA_{MM}^2}{4\lambda^2}, \tag{1}$$

where $V_{MM}$ is the normalized frequency from waveguide theory [12, 13]. This specifies the number of cores $N_{SM} = N_{MM}$ required in the MCF, given a design for the MMF.

There is no simple exact expression for the number of MMF modes, but the $N \approx V^2/4$ formula in Eq. (1) has the correct asymptotic behavior and a sound physical basis [12, 13]. Each of the spatial modes it counts has two polarization states. If these are counted separately both $N_{MM}$ and $N_{SM}$ are multiplied by 2 (since each "single-mode" core also supports two polarizations), so it doesn't matter whether spatial modes or polarization modes are counted as long as we are consistent. We choose to omit the factor of 2 and count spatial modes, so that $N_{SM}$ is simply the number of SM cores.

A mode-number mismatch $N_{SM} \neq N_{MM}$ normally causes loss at whichever taper transition sees $N$ decreasing. If all input MMF modes are equally excited, the expected loss corresponds to the number of discarded degrees of freedom in that transition [1]:

$$loss = \left| 10 \log_{10} \left( \frac{N_{MM}}{N_{SM}} \right) \right| dB. \tag{2}$$

Note that $N_{MM}$ in Eq. (1) depends on $\lambda$ whereas $N_{SM}$ is obviously fixed, so mode-number matching is only possible at a single wavelength. (A MCF could be designed with successive cores becoming two-moded as wavelength decreases, so as to preserve mode-number matching over a wide spectrum, but FBG devices require SM cores.) Fig. 2(a) shows the wavelength dependence of the loss from Eq. (2) given the $\lambda$ dependence in Eq. (1).

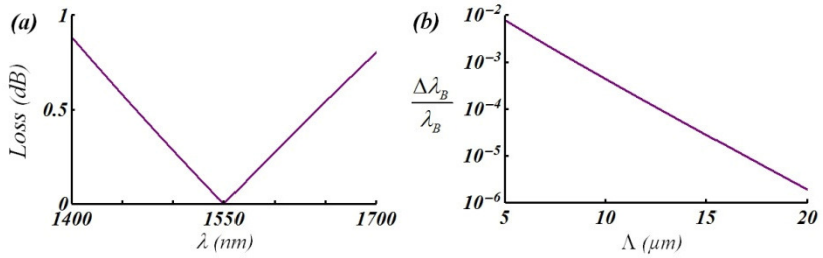


Fig. 2. (a) Calculated mode-number mismatch loss for a lantern device designed for $\lambda$ = 1550 nm operation, if all input modes are equally excited. (b) Calculated $\Lambda$ dependence of supermode splitting for a MCF with $NA$ = 0.22, $\lambda$ = 1550 nm and $d$ = 3.9 μm, where $\Lambda$ is the core spacing.

We opted for a mode-number matched design. However, since differential losses in long MMFs deplete the power in the modes closest to cutoff [14], it may be better to make $N_{SM}$ slightly less than $N_{MM}$. The MMF modes lost in the first transition will carry little light anyway, and the excess of MMF modes at the end of the second transition allows it scope to be low loss over a broader wavelength range.

#167650 - $15.00 USD Received 30 Apr 2012; revised 22 May 2012; accepted 28 May 2012; published 8 Jun 2012

*2.2 Fibre Bragg grating uniformity*

A FBG reflects light with wavelengths satisfying a Bragg condition, relating the propagation constant $\beta$ of the guided mode to the grating's Fourier components [4, 5, 15]. To reproduce an SM response in a photonic lantern device, the light in all the MCF's cores must see the same FBG response. For example, the original astronomical application of photonic lanterns is for the suppression of OH emission from the upper atmosphere. The widths and positions of the emission lines require the filter wavelengths to match to within $\Delta\lambda \approx 160$ pm [4], which we take to be our target tolerance. Assuming the same grating index modulation imprinted on all cores, this requires the cores themselves to be identical and optically isolated from each other. Variations in diameters $d$ and/or numerical apertures $NA$ gives rise to differences in $\beta$ and hence a core-to-core spread of Bragg wavelengths $\lambda_B$. Manipulation of expressions for fundamental-mode $\beta$ [12] leads to

$$\frac{\Delta\lambda_B}{\lambda_B} = \left(\frac{NA}{n_0}\right)^2 \left\{\eta\frac{\Delta NA}{NA} + \left(\eta - \frac{W^2}{V^2}\right)\frac{\Delta d}{d}\right\}, \tag{3}$$

where $\Delta x$ represents a small spread in any parameter $x$'s value, $W$ is the cladding parameter [12], $\eta$ is the fraction of mode power in the SM core and $n_0$ is the refractive index of silica. A small correction due to material dispersion is neglected and $(NA/n_0)^2 << 1$ is assumed. Both $W/V$ and $\eta$ take values between 0 and 1, are universal functions of the SM core's normalized frequency $V$, and can be found from modal solutions such as those in [12]: for a typical $V = 2$, the coefficients of $\Delta NA/NA$ and $\Delta d/d$ in Eq. (3) are 0.741 and 0.235 respectively. The key result of Eq. (3) is therefore that the relative sensitivity of $\lambda_B$ to core variations scales as $NA^2$.

Bending of the MCF also induces a $\beta$ variation [16], which depends on the width $D$ of the array of cores and the bend's radius of curvature $R$ and leads to

$$\frac{\Delta\lambda_B}{\lambda_B} = (1+\chi)\frac{D}{R} = \left(\frac{2\sqrt{3}}{\pi}\right)^{1/2}\frac{(1+\chi)\Lambda\sqrt{N_{SM}}}{R}, \tag{4}$$

where $\chi = -0.22$ for silica [16], $\Lambda$ is the center spacing (or pitch) of the SM cores, and $N_{SM}$ should match $N_{MM}$ in Eq. (1). $\Lambda$ in Eq. (4) was related to $D$ geometrically, assuming that the cores lie on a triangular lattice with a roughly-circular outer boundary:

$$D = \left(\frac{2\sqrt{3}}{\pi}\right)^{1/2}\Lambda\sqrt{N_{SM}}\,. \tag{5}$$

Isolation of the cores from each other is necessary to avoid supermode splitting. The normal modes of an array of coupled cores are combinations - supermodes - of the modes of the individual cores with fixed amplitude and phase relationships. The supermode $\beta$ 's are split by an amount related to the strength of coupling, which depends on $\Lambda$ and the extent of the evanescent fields. Again this can be related to a $\lambda_B$ spread using results from [12]:

$$\frac{\Delta\lambda_B}{\lambda_B} = \frac{9}{2n_0^2}\left(\frac{\lambda V}{W}\frac{NA^3}{\Lambda}\right)^{1/2}\frac{U^2}{V^4 K_1^2(W)}\exp\left(-\frac{2\pi W}{\lambda V}\frac{\Lambda NA}{}\right), \tag{6}$$

Where $U$ is the core parameter [12] and $K$ is the modified Bessel function, the exponential factor being dominant. An example of the variation of $\Delta\lambda_B/\lambda$ with $\Lambda$ is shown in Fig. 2(b).

Equations (3)-(6) give the spread in Bragg wavelengths $\lambda_B$ due to various imperfections, or indicate tolerances for those imperfections given a maximum tolerable $\lambda_B$ spread. Equation

#167650 - $15.00 USD Received 30 Apr 2012; revised 22 May 2012; accepted 28 May 2012; published 8 Jun 2012

(6) tells us that large values of Λ and *NA* reduce supermode splitting. However, Eq. (3) shows that large *NA* increases sensitivity to core-to-core variations of *d* and *NA* (which in practice may be hard to control) and Eq. (4) shows that large Λ increases sensitivity to bending. Bend sensitivity is probably the simplest to mitigate, by holding the MCF straight, in which case low *NA* in Eq. (6) can be countered by large Λ. The disadvantage of this approach is that it can make the array of cores (and hence the entire fibre) very large, Eq. (5).

*2.3 Taper transition*

As well as mode-number matching, for low loss the taper transition must also be long enough to be adiabatic. Each MMF mode evolves into a supermode of the SM array, and vice versa, without coupling to cladding or radiation modes. (To be precise, coupling to other supermodes is acceptable.) Adiabaticity criteria are well known for single cores, and generalize to MCFs. For example, the "weak power transfer" criterion for low loss in a waveguide transition [17] with an alternative form for the local-mode coupling coefficient [12] has the form:

$$\left| \frac{2}{\beta_1 - \beta_2} \int \Psi_1 \frac{\partial \Psi_2}{\partial z} dA \right| << 1, \tag{7}$$

where $\Psi_j(x, y)$ are the normalized field distributions of modes $j = 1, 2$ between which power transfer may occur, the $z$ axis lies along the fibre and the integral is over the transverse cross-section spanned by the $x$ and $y$ axes. The intuitive result is that loss is more likely where mode field distributions change rapidly along the transition, so sudden changes in mode shape should be avoided.

To be quantitative, we simulated a complete MCF lantern (with no FBGs) using the beam propagation method (BPM) [18]. The BPM code only finds a maximum of 100 modes so our model, Fig. 3, has 85 step-index SM cores with $NA_{SM} = 0.22$ and $d = 3.9$ μm in a triangular array with $\Lambda = 16.9$ μm in a MCF cladding of diameter 186 μm and index $n_0 = 1.44$. The fibre tapers within a low-index jacket material to give MMF ports with $NA_{MM} = 0.234$ and $d_{MM} = 38.83$ μm. $N_{MM} = 90$MMF modes were found for $\lambda = 1550$ nm, slightly more than the $N_{SM} = 85$ SM cores, so Eq. (2) predicts a mode-number mismatch loss of 0.25 dB. (The discrepancy was partly due to the residual tapered-down SM cores of the MCF, which are too small to guide light but slightly increase the average index of the MMF core.) Figure 3(c) shows a BPM simulation of the field of a typical MMF mode as it propagates along the input transition. As the MCF gets bigger the light in the mode gradually becomes concentrated in the enlarging SM cores, to form a supermode pattern in the full-sized MCF. A reverse change occurs along the output transition.

Figure 3(d) shows how the loss of the complete device depends on the length $L$ of the transitions. An input field was set up by summing all 90 MMF modes with equal amplitudes and random phases. Its propagation through the complete lantern of Fig. 3(a) was simulated by BPM for various $L$. The overlaps of the output field with the guided modes were calculated and their square-moduli summed to give the overall transmission. Together with index-matching of the jacket material in the central section of the structure, this ensures that only guided light is included when calculating transmission. For $L \geq 2$ cm the loss was < 0.35 dB, giving a transition loss through both tapers of < 0.1 dB when the mode-number mismatch loss of 0.25 dB is subtracted. Thus realistically-long transitions can yield very low loss.

This appears to contradict [3] which concluded that the SM cores must be at least $\Lambda = 60$ μm apart for low loss, much more than the $\Lambda \approx 17$ μm of our simulation and experiments. The discrepancy is because [3] considered an array of seven SM cores with various Λ but always the same cladding diameter of 110 μm. Small Λ therefore means that the array of cores occupies only a small region at the center of the fibre, leaving the rest of the fibre empty of

#167650 - $15.00 USD Received 30 Apr 2012; revised 22 May 2012; accepted 28 May 2012; published 8 Jun 2012

cores. When such a fibre is tapered, the field must rapidly expand from the small central array of seven cores to fill the entire fibre, a dramatic change causing high loss, Eq. (7). In contrast, the MCF in Fig. 3 has cores distributed throughout the fibre. When it is tapered, the field in each core only needs to expand enough to occupy its own "unit cell" in the cross-section, a much more gradual change of field shape. Thus the high loss reported in [3] was due to an unrepresentative feature in the modeled MCF.

Figure 3(c) graphically illustrates a key point about lantern transitions: they are not mode demultiplexers that couple each MMF mode into just one of the SM cores. As long as the light ends up in SM cores, it doesn't matter how many of them it's distributed between.

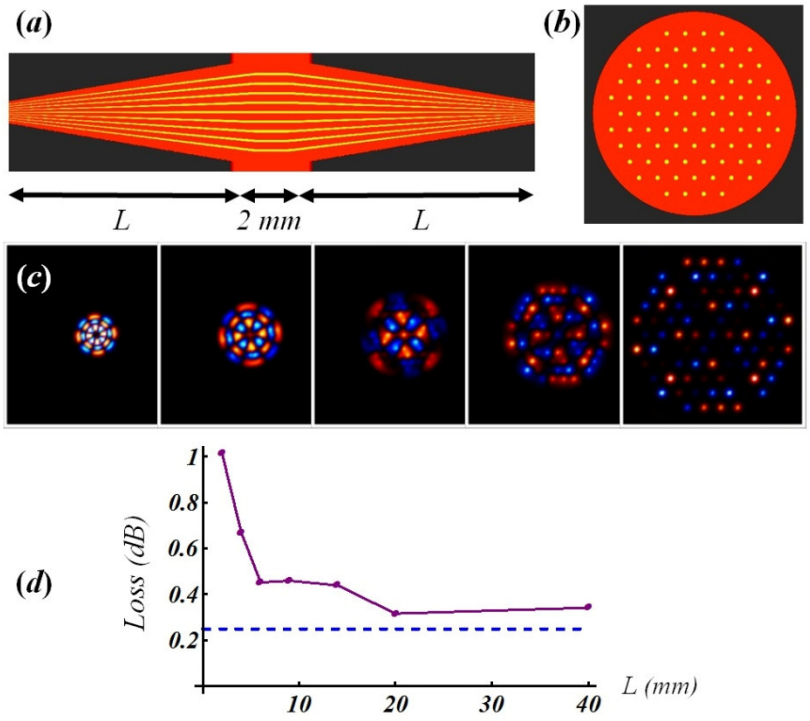


Fig. 3. (a) Side view of a model MCF lantern. The transitions are surrounded by depressed-index material (shown black) along most of their lengths to mimic a MMF at the ends, but the central section (including 2 mm of uniform fibre) is surrounded by matched-index material (shown orange) to strip away cladding modes. (b) Cross-section of the 85-core MCF. (c) BPM simulation of an $LP_{4,3}$-like MMF mode propagating along the left transition: red and blue represent opposite phases. (d) Simulated $L$ dependence of loss. The broken blue line represents 0.25 dB of mode number mismatch loss. Lengthening the uniform section to 10 mm had < 0.02 dB impact on the loss for $L$ = 4 mm.

## 3. Experiment

### *3.1 Multicore fibres*

Our chosen MCF design for $\lambda$ = 1550 nm had $N_{SM}$ = 120 Ge-doped cores with $d$ = 3.9 µm, $\Lambda$ = 16.9 µm and $NA$ = 0.22 within an undoped silica cladding of outer diameter 230 µm. These cores had $V$ = 1.74 and a supermode splitting of $\Delta\lambda_B$ = 16 pm from Eq. (6). To keep within the target wavelength spread of $\Delta\lambda_B$ = 160 pm [4], the diameter tolerance of the SM cores is 1.3% from Eq. (3) and the minimum bending radius is 1.5 m from Eq. (4). From Eq. (1), the MCF supports the same number of modes as a step-index MMF with $d_{MM}$ = 50 µm and $NA_{MM}$ = 0.215. Ports compatible with such a MMF can be formed by jacketing the MCF with a

#167650 - $15.00 USD Received 30 Apr 2012; revised 22 May 2012; accepted 28 May 2012; published 8 Jun 2012

suitable depressed-index F-doped silica capillary, then tapering it down to 0.22 × its original diameter (see Section 3.3).

The Ge-doped silica for the SM cores came from a commercially-available MMF preform [19]. Its specified diameter tolerance was ~2.5% but manufacturer's data indicated a variation of less than 1% over half its length. This preform was drawn to rods of 1 mm diameter. A rod was inserted into each capillary in a stack of 121 undoped silica capillaries. The first such stack used rods from the uniform part of the Ge-doped preform and was drawn directly to give fibre A, Fig. 4(a). (One core was deliberately omitted from this fibre, by replacing a doped rod with an undoped rod, to act as an index mark. Fibre A therefore had $N_{SM}$ = 120 cores. The site of the missing core is partly obscured by the cleave in Fig. 4(a) but can be seen at the top of the jacketed fibre in Fig. 7(b).) A second similar stack, but with no missing core and $N_{SM}$ = 121, included rods from the less-uniform part of the Ge-doped preform. It was drawn to intermediate canes which were jacketed with undoped silica then drawn again to give fibre B, making fibre B's outer diameter 400 µm for a similar array of SM cores, Fig. 4(b).

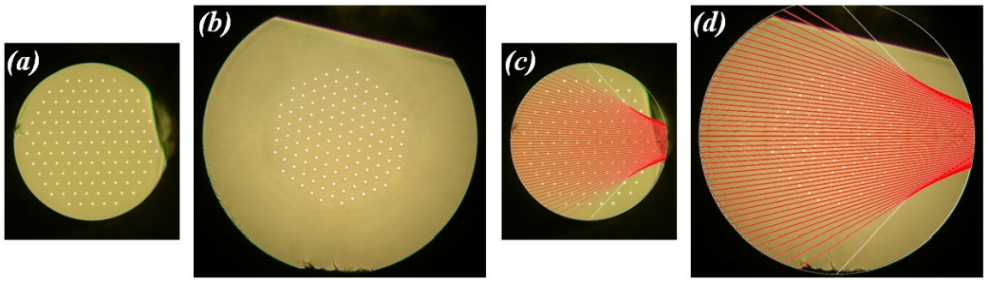


Fig. 4. Optical micrographs (to the same scale) of (a) fibre A and (b) fibre B. The diameter of fibre A is 230 µm. The flat edges are due to imperfect cleaving. (c, d) Micrographs (a, b) overlaid with ray traces for a plane wave incident from the left. The focused wave overlaps all the cores in (d) but avoids some cores in the upper- and lower-right of (c).

The average attenuation of fibre A was measured by the cutback method, with 1550 nm light coupled into all of the cores, to be between 0 and 0.025 dB/m. (Precision was limited by the short length measured, and in any case only ~1 m of the fibre is needed for one device.) The core pitch was $\Lambda$ = 17.5 µm, slightly bigger than intended. The second-mode cutoff wavelength of the SM cores was found by the mandrel technique to be 1170 nm, within 10 nm of the design value when scaled with the increased pitch. To assess supermode splitting, we looked for directional coupling for input light in just one core. The intensity in adjacent cores relative to that in the central core was <10% for 0.25 m of fibre and >50% for 0.75 m of fibre. A coupling length of this order corresponds to a supermode splitting of the order of $\Delta\lambda_B$ ~10 pm, consistent with the design value.

### *3.2 Fibre Bragg gratings*

One major advantage of the multicore lantern concept is that the FBGs are written in one go across all the cores of the MCF. However, to our knowledge the maximum number of MCF cores in which FBG inscription has been previously reported was four [7, 8]. To form the complex FBGs required for OH suppression, which have only ever been demonstrated by one research team anyway [5], would have been an additional complication that we were not equipped to solve. We therefore explored the principle of the MCF lantern by writing simple single-notch FBGs across the >100 cores of fibres A and B.

The procedure for writing the FBGs was unchanged from that normally used to write FBGs in ordinary SM fibres [15]. Lengths of MCF were hydrogen-loaded for two weeks at room temperature and 20 bar pressure, before inscription of the gratings by a UV laser beam

#167650 - $15.00 USD Received 30 Apr 2012; revised 22 May 2012; accepted 28 May 2012; published 8 Jun 2012

of power 100 mW, diameter 0.7 mm and wavelength 244 nm through a phase mask of period 1067 nm. The beam was scanned along 5 cm of the MCF at 21 μm/s. No attempt was made to orient the fibre's core pattern with respect to the direction of the UV beam.

Each tested MCF was cleaved at both ends to access all its cores, and held straight between supports. To characterize the FBGs' transmission spectra, Fig. 5, a photonic crystal fibre (PCF) generating supercontinuum light was butt-coupled to the MCF. The near field at the output of the MCF was imaged by a microscope objective onto a screen ~50 cm away. The image was focused and positioned by translating the objective, approximately by eye (using the visible components of the supercontinuum light) and then precisely for the infrared light of interest with the aid of an InGaAs camera with a 1550 nm bandpass filter. The entire pattern of cores was illuminated by widening the gap between PCF and MCF, or a particular core selected by closing the gap and transverse positioning. (The index mark in fibre A identified corresponding cores in different pieces of fibre.)

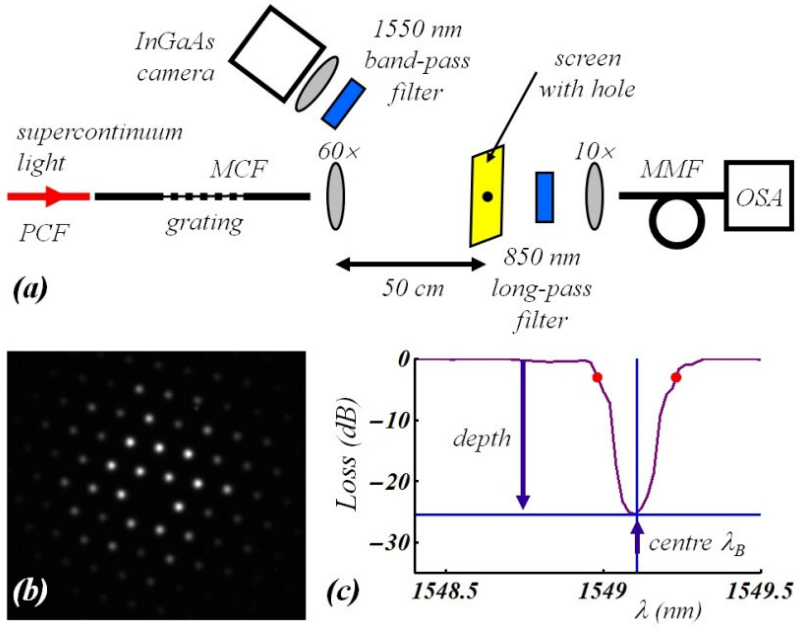


Fig. 5. (a) Experimental setup used to measure the grating spectra in each MCF core - see text for details. (b) Typical IR near-field image of the MCF output when several cores were illuminated. The absent core image near the center of the pattern overlies the hole in the screen. (c) A typical normalized grating loss spectrum, indicating the grating depth and center wavelength (bisecting 3 dB points).

Light from a chosen core passed through a hole in the screen and was focused into a multimode collection fibre. Its transmission spectrum was measured using an optical spectrum analyzer (OSA). The OSA lacked an order-sorting filter, so a long-pass filter with an edge at 850 nm was placed between screen and multimode fibre. The FBG notches were narrow and the background signal (away from the notches) was flat, so it was not necessary to take reference measurements. The background level was simply interpolated across the notch and subtracted to give a normalized response, Fig. 5(c), from which the notch's depth and center wavelength $\lambda_B$ were extracted. (From the observed flatness of the background signal, we estimate that the normalization process introduced no more than ± 0.4 dB of uncertainty to the extracted notch depth values.) This process was repeated for each of the 120 or 121 cores.

Maps of notch depth and center wavelength for 5 samples are shown in Fig. 6. Referring to the parts of the figure, (a) and (b) are typical results for fibre A. Although the strengths of

#167650 - $15.00 USD Received 30 Apr 2012; revised 22 May 2012; accepted 28 May 2012; published 8 Jun 2012

the FBGs varied from sample to sample, in all cases there were definite notches in most cores but two margins with no notches (rows of red dots in the upper maps). The orientation of the margins in the maps changed between samples but the patterns were always very similar. We attribute this pattern to focusing, by the curved outer surface of the fibre, of the UV beam used to write the FBGs [8]. A simple ray trace across a silica cylinder for an incident plane wave is overlaid on an image of fibre A in Fig. 4(c). The two regions avoided by the rays resemble the margins in the FBG maps. The varying orientation of the margins is simply because the orientation of the fibre in the FBG writing rig was random from sample to sample.

The variations in the notch center wavelength $\lambda_B$ in Fig. 6(a) and 6(b) correlate with the variations in notch depth rather than with the absolute position in the fibre, and were more pronounced in samples with stronger gratings. The wavelength spread was therefore due more to uneven FBG inscription than to differences between the cores themselves from imperfect fibre fabrication. The standard deviation of $\lambda_B$ was 100 pm for (a) and 67 pm for (b).

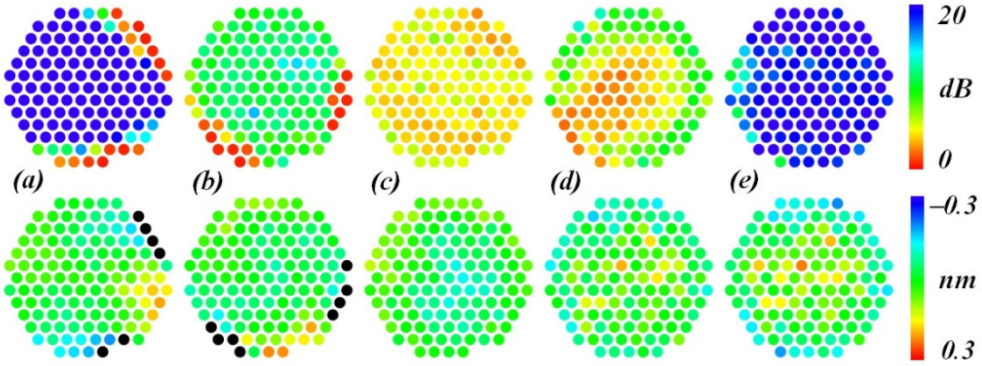


Fig. 6. Maps of (upper) notch depth and (lower) offset of center wavelength $\lambda_B$ from the mean, for the FBGs in (a-c) three samples of fibre A and (d-e) two samples of fibre B. Each colored dot in a map summarizes the FBG in one core of the MCF, at the corresponding location in the fibre cross-section. The maps are oriented (and if necessary reflected) so that each core is in the same position for each fibre: the missing core is at the end of the bottom row in (a-c), and distinct patterns of cores with anomalous $\lambda_B$ are co-aligned in (d-e).

Although these results show that FBGs can indeed be written across >100 cores in one shot, it is undesirable for some cores to lack FBGs. Even one core without a FBG will transmit enough unfiltered light to limit the notch depth of an otherwise-perfect photonic lantern filter to 21 dB. We attempted two methods to mitigate the effects of UV focusing. For sample (c) we immersed the exposed section of fibre A in index-matching oil when writing the grating. A silica microscope cover slip was placed between fibre and phase mask to form a flat interface that eliminated focusing while keeping the oil off the phase mask. The resulting FBGs had very shallow notches, Fig. 6(c), but there was a FBG in every core. We believe the shallow notches were due to absorption of UV light in the oil, and could be improved by selecting a fluid more transparent to UV light (or a longer or more intense UV exposure). The standard deviation of $\lambda_B$ was 57 pm, the smallest of all the samples measured, showing that core uniformity in the MCF itself was good enough to make lantern filters suitable for OH suppression.

The second way to mitigate UV focusing was to make a new MCF with a uniform silica outer cladding: fibre B, Fig. 4(b). This ensured that the entire array of SM cores was more central and so overlapped with the UV field, Fig. 4(d). Samples (d) and (e) in Fig. 6 were made from this fibre, (e) being exposed to UV light for more time than (d). Again there was a FBG in every core, though the distribution of notch depths was not as uniform as (c). In particular there is evidence of a core shadowing effect in (d), whereby cores further from the

#167650 - $15.00 USD Received 30 Apr 2012; revised 22 May 2012; accepted 28 May 2012; published 8 Jun 2012

UV source have weaker FBGs because some of the light is absorbed or scattered by nearer cores (in which case we assume the UV light approached from the top-right). This could be reduced by increasing Λ to give the fibre a lower filling fraction of core to cladding glass - perhaps another design principle to add to those in Section 2.

We can also see that $\lambda_B$ uniformity was poor, and indeed there was a distinct pattern of cores with anomalous $\lambda_B$ which persisted across a total of 7 samples with the same fibre. Since the orientations of the fibres during grating inscription were random, we attribute the deviations to variations in the MCF's cores themselves. This is not surprising, since fibre B was made with core rods from the less-uniform section of the original MMF preform (Section 3.1).

Other possible methods to prevent UV focusing include giving the fibre a flat side (a D-shaped or even square outer boundary), during fabrication or by side-polishing afterwards.

*3.3 Taper transitions*

The MCF was tapered down to form transitions to interface the FBGs to the input and output MMFs. If tapered to a small-enough size the SM cores cease to be good waveguides, the light being guided instead by the fibre's outer boundary if the outside medium has a lower refractive index than the MCF's cladding. By using F-doped silica (with a lower index than undoped silica) as the outside medium, the entire tapered-down MCF resembles the core of a MMF, with the F-doped silica as the cladding.

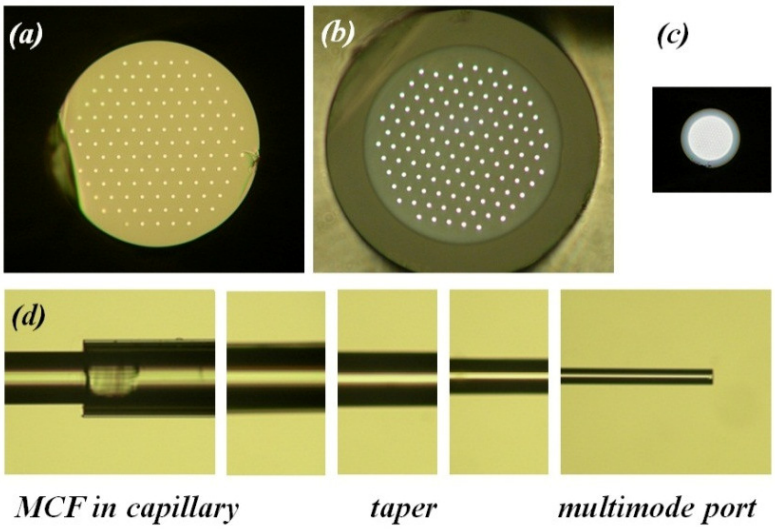


Fig. 7. (a-c) Cross-sectional optical micrographs (transmitted illumination, to the same scale) of (a) uncoated fibre A with outer diameter 230 μm, (b) fibre A jacketed with F-doped silica and (c) the jacketed MCF tapered down to mimic a MMF with a 50 μm core. (d) Montage of side-view micrographs of the transition.

A convenient form of this structure would be a MCF with the F-doped silica built-in as an outer cladding, around an undoped inner cladding containing the SM cores. The fibre could then be tapered without further steps to form the MMF ports. Indeed the outer cladding would help FBG inscription as discussed in Section 3.2, like the undoped outer cladding of fibre B. However, such a fibre is unlikely to yield good FBG filters. All light passing the FBGs should be guided by the SM cores, so that the unwanted OH lines are reflected. However, no taper transition is perfectly adiabatic: there will always be some mode coupling to the MCF's cladding modes. This light is not filtered by the FBGs and can persist to the output MMF, allowing up to 10% of the light in a lantern of just 0.5 dB loss to be transmitted unfiltered,

#167650 - $15.00 USD Received 30 Apr 2012; revised 22 May 2012; accepted 28 May 2012; published 8 Jun 2012

and reducing the filter's extinction to less than 10 dB even if the FBGs were perfect. It is therefore important to expose the MCF's inner cladding to an external medium (such as a standard high-index polymer coating) that strips away any cladding light that bypasses the FBGs.

We therefore locally gave the MMF ports a depressed-index cladding by tapering the bare MCF inside a capillary. The capillaries had inner and outer diameters of 270 µm and 360 µm respectively, and were drawn from an F-doped silica tube with NA = 0.21 relative to undoped silica. After FBG inscription, several centimeters of 230 µm diameter fibre A were stripped of coating at one end, cleaned with acetone and threaded through a 45 mm long piece of the capillary. The fibre was mounted on the tapering rig so that the capillary was suspended on the fibre between the clamps. An oxy-butane flame was passed slowly along the central 25 mm of the capillary, while the stages holding the fibre moved 1.2 mm further apart (enough to keep the fibre straight without narrowing it much). The flame softened the capillary and made it shrink onto the fibre by surface tension, Fig. 7(b). The softening temperature of the F-doped silica was estimated to be over 200 °C below that of undoped silica [20], so the MCF was not significantly deformed by the process. (Attempts - motivated by curiosity - to similarly collapse undoped silica onto the fibre required higher temperatures and invariably caused deformation and high losses.)

The jacketed fibre was remounted in the tapering rig so that both capillary and fibre were clamped at both ends. The fibre was heated and stretched faster than before to reduce its diameter to 50 µm over transitions 20 mm long, Fig. 7(d). The waist of the tapered structure was then cleaved with a ceramic tile to yield a MMF port, Fig. 7(c), connected to the FBG region by a length of coated MCF that provides the cladding-mode stripping function discussed previously. The other half of the structure, attached to a few centimeters of bare MCF, could be inspected to check the quality of the cleave.

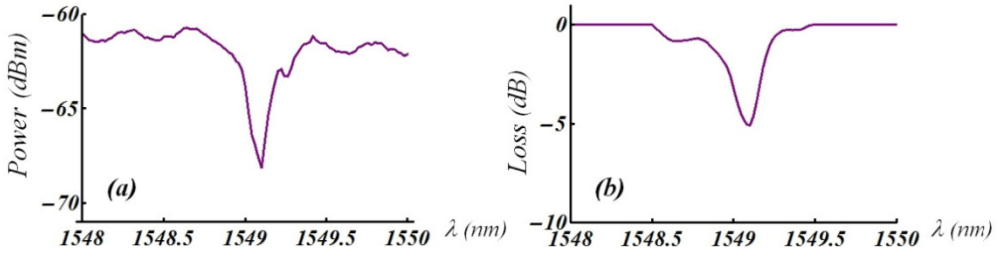


Fig. 8. (a) Un-normalized transmission spectrum of a complete lantern device made from a length of MCF with the FBGs of Fig. 6(b). (b) Linear-average loss spectrum calculated from the FBG spectra summarized in Fig. 6(b).

The process was then repeated on the other side of the FBG region to form a complete photonic lantern filter. For the device with the FBGs shown in Fig. 6(b), the measured un-normalized transmission spectrum between input and output MMF ports is plotted in Fig. 8, along with the calculated average of the measured transmission spectra in the 120 cores of the MCF. The measured spectral notch is only ~7 dB deep, which is not a good extinction for a FBG. However, this poor extinction is due to the uneven distribution of notch depths and center wavelengths across the SM cores. Indeed, the presence of 12 cores with no noticeable grating notches at all, Fig. 6(b), would reduce the maximum extinction to 10 dB even if the remaining gratings were perfect. If the distribution of FBGs was more uniform, for example following development of the methods discussed towards the end of Section 3.2, then a correspondingly improved lantern transmission spectrum would result.

We have not measured the insertion loss of the lantern filter, because of the difficulty of obtaining a reliable reference measurement without (for example) splicing a length of matched MMF onto the input to allow a cutback. However, expected losses were estimated by

#167650 - $15.00 USD Received 30 Apr 2012; revised 22 May 2012; accepted 28 May 2012; published 8 Jun 2012

measuring the powers transmitted by meter lengths of fibre A before and after tapering, for 1550 nm light coupled into all of the cores. In four experiments using our most successful process, the loss of the complete biconically-tapered jacketed MCF was <0.5 dB, of which <0.1 dB arose from jacketing with the F-doped capillary. Although the structure was the converse of a lantern (ie, MCF-MMF-MCF instead of MMF-MCF-MMF), both incorporate the same transitions (one up-taper and one down-taper) and should have similar losses.

## 4. Mode scrambler

The photonic lantern structure of Fig. 1 (but without the FBGs in the SM cores) has interesting properties of its own. During the experiments described above we noticed that the lantern filter was also a very effective mode scrambler [14].

In an ordinary MMF, a monochromatic input wave coherently excites a spectrum of modes. These acquire relative phase differences from their dissimilar propagation constants $\beta$. The intensity distribution across the end of the MMF therefore differs from that at the input. To randomize the phases and make the output incoherent, it is necessary either to give the light a large enough bandwidth and exploit the wavelength dependence of the modes ' $\beta$ 's and differential group delays, or to continuously disturb the fibre and time-average the output. Even so, this only changes the phases of the modes and not their amplitudes.

In contrast, the input transition of our photonic lanterns effectively samples the input MMF pattern spatially to deliver it into the SM cores of the MCF, Fig. 3(c).The light propagates independently in the $N$ cores, inevitably experiencing different phase changes due to bends in the MCF and dissimilarities between the cores. This couples light between the degenerate supermodes of the MCF and hence the modes of the output MMF, scrambling the modal amplitudes as well as their phases. A suitable perturbation should then yield an incoherent and uniform mode spectrum. The operation of the transitions resembles a Fourier transform, transforming light between states of definite spatial frequency (MMF modes) and states of definite spatial position (MCF cores), these states additionally suffering random phase changes due to propagation along their respective waveguides. The resulting repeated convolutions thoroughly scramble the modes. (This Fourier analogy becomes almost exact in the hypothetical case of a square array of cores.)

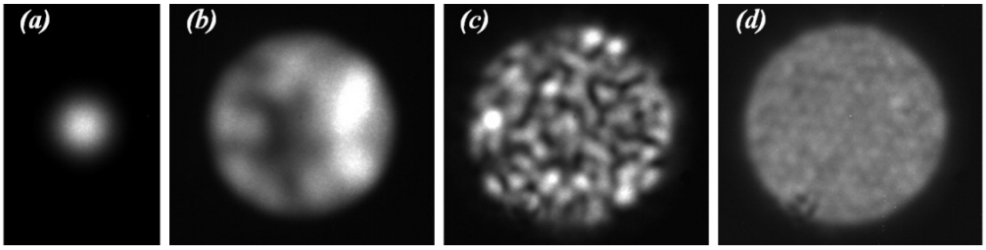


Fig. 9. Near-field images at 1550 nm (time constant ~30 ms) at the output of (a) a graded-index MMF butt-coupled to (b) a step-index MMF (Media 1) or (c) a MCF photonic lantern with similar step-index MMF ports (Media 2). (d) repeats (c) while the fibre was disturbed by hand and the camera time constant was 0.1 s. The media for (b) and (c) are corresponding movies where a loop of the fibre was gently oscillated.

A photonic lantern with ~2 m of fibre A between the transitions was held so that a ~1 m loop of the MCF hung off the edge of the table. Light from a 1550 nm diode laser was coupled into a graded-index MMF with a 62.5 µm core, favoring the fundamental mode, Fig. 9(a). The output of this fibre was butt-coupled to the input MMF port of the lantern (core diameter 50 µm, NA = 0.21). The output MMF port was imaged in the near field using the InGaAs camera. The experiment was repeated with a similar length of a step-index MMF (with the same core diameter and NA) instead of the MCF lantern, again with the input wave shown in Fig. 9(a). Static images in both cases are shown in Fig. 9(b, c), with links to movies

#167650 - $15.00 USD Received 30 Apr 2012; revised 22 May 2012; accepted 28 May 2012; published 8 Jun 2012

where the hanging fibre loop was oscillated with an amplitude of about 10 cm by gentle air movement. Figure 9(d) is a time-averaged image where the MCF was disturbed more vigorously (but still quite gently) by hand.

The pattern at the output of the lantern, Fig. 9(c), had a high spatial frequency similar to that expected for modes close to cutoff in a MMF guiding 120 modes. In contrast the pattern at the output of the simple MMF, Fig. 9(b), had a much lower spatial frequency matching that of the input field, Fig. 9(a). This suggests that (as expected) power in this short MMF was not significantly coupled from the restricted set of modes initially excited, whereas the lantern distributed light across the full spectrum of guided modes.

The movies demonstrate that phase scrambling as a function of time for a given disturbance was much stronger in the lantern than in a similar length of step-index MMF. The pattern in Fig. 9(d), time-averaged over 0.1 s, shows how readily a modest perturbation can wash out all interference between the guided modes, even with a laser source. Indeed the illumination in Fig. 9(d) was so uniform and incoherent that the pattern of residual SM cores in the lantern's tapered-down MMF core can be discerned.

## 5. Conclusions

We have described the design and fabrication of the first photonic lantern made from multicore fibre. Key design principles for narrow spectral filters were identified, principally to limit spectral non-uniformities due to dissimilarities between the cores, supermode splitting (if the cores are too close) and bending. A beam propagation analysis showed that, contrary to assertions elsewhere, low-loss taper transitions are possible in multicore fibres with realistic core separations.

Fibre Bragg gratings were simultaneously written across all 120 cores of a MCF designed for a lantern-based spectral filter matching a typical step-index multimode fibre, greatly exceeding the previously-reported numbers of cores for which FBG inscription was reported. Good uniformity of Bragg wavelengths across the cores was demonstrated. Focusing by the curved fibre surface of the UV beam that wrote the gratings caused large variations in grating notch depth between the cores, and we explored two approaches to mitigating this problem.

Complete photonic lantern structures were formed by tapering a MCF inside a doped silica capillary with a depressed refractive index, so that the tapered structure mimics a multimode fibre whose core is the entire tapered-down MCF. The expected loss of the structure was <0.5 dB. FBG non-uniformities account for the poor extinction of the final lantern filter, and much improved results should be possible given successful further development of the methods identified for countering the effects of UV beam focusing.

The multicore photonic lantern (without gratings) also functions as a very effective mode scrambler, randomly distributing phase and amplitude among all the guided modes of the output multimode fibre.

## Acknowledgments

The authors thank R. Thomson, J. Bland-Hawthorn, S. G. Leon-Saval and R. Haynes for stimulating discussions, and the innoFSPEC, Leibnitz-Institute for Astrophysics Potsdam for providing glass for fibre fabrication. T. A. Birks thanks the Leverhulme Trust for a Research Fellowship. A. Díez and J. L. Cruz acknowledge the Ministerio de Educación y Ciencia of Spain for financial support (project TEC2008-05490). D. F. Murphy acknowledges funding from Enterprise Ireland.

#167650 - $15.00 USD Received 30 Apr 2012; revised 22 May 2012; accepted 28 May 2012; published 8 Jun 2012